

Validation of Shielded Cable Modeling in Xyce Based on Transmission-line Theory

Salvatore Campione*, Aaron J. Pung, Larry K. Warne, William L. Langston, Ting Mei, and Howard G. Hudson

Abstract—Cables and electronic devices typically employ electromagnetic shields to prevent coupling from external radiation. The imperfect nature of these shields allows external electric and magnetic fields to induce unwanted currents and voltages on the inner conductor by penetrating into the interior regions of the cable. In this paper, we verify a circuit model tool using a previously proposed analytic model [1], by evaluating induced currents and voltages on the inner conductor of the shielded cable. Comparisons with experiments are also provided, aimed to validate the proposed circuit model. We foresee that this circuit model will enable coupling between electromagnetic and circuit simulations.

1. INTRODUCTION

Isolating electrical components from unexpected radiation is a challenging task. Demonstrated solutions include wire-mesh shields [2], material shielding [3], metallic enclosures [4], and braided shields [5]. The quality of each shield is gauged by its ability to reduce the electromagnetic field at a given point in space caused by placing a shield between the source and that point, also known as the shielding effectiveness (SE) [6–9]. A formulation of the transmission-line model of multiple shielded cables was presented in [1] for a cable with arbitrary terminations. This geometry is illustrated in Figure 1.

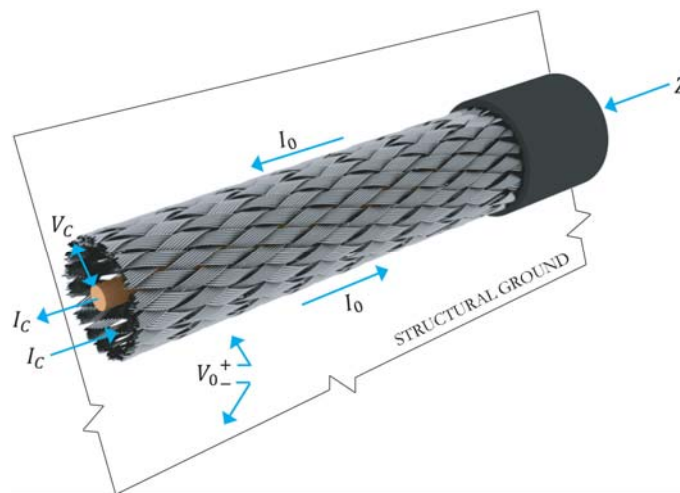


Figure 1. Illustration of the geometry of a shielded cable and its associated voltages and currents.

Received 3 June 2019, Accepted 26 August 2019, Scheduled 5 September 2019

* Corresponding author: Salvatore Campione (sncampi@sandia.gov).

The authors are with the Sandia National Laboratories, Albuquerque, NM 87123, USA.

In this paper, we develop a circuit model to evaluate currents and voltages induced on the inner conductor of a braided-shield cable, using the analytic model in [1]. The circuit model demonstrates a combined electromagnetic-circuit capability, and can be modeled by any SPICE-like analysis tool. For this work, we use the AC analysis in frequency domain provided by the Xyce Parallel Electronic Simulator [10], developed at Sandia National Laboratories.

Although we currently employ braided-shield parameters using Kley's semi-empirical model for EM coupling through a braided shield [11], circuit model parameters that account for the cable geometry can be computed using a first principles multipole model [12–14]. This can be particularly useful if perturbations exist in the shield geometry versus nominal commercial braid parameters.

2. CIRCUIT IMPLEMENTATION OF THE SHIELDED CABLE

Based on the transmission-line model, per-unit-length circuits for the outer shield and inner conductor are shown in Figure 2. The time harmonic dependence $\exp(j\omega t)$ is implicitly assumed here. Each circuit has length Δz , representing a single unit cell of a cable with N individual cells. A traveling current/voltage wave I_0/V_0 is injected on the shield (often in applications, this might be induced by an external drive field). The outer braid is characterized by a per-unit-length shield admittance Y_0 and shield impedance Z_0 .

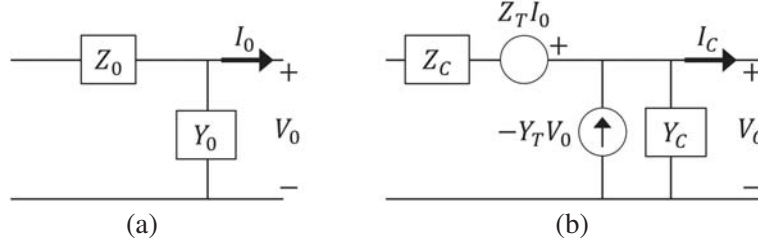


Figure 2. Per-unit-length transmission line circuits are shown for (a) outer shield and (b) inner conductor.

Through field penetration, some currents and voltages will be induced on the inner conductor. The inner conductor is defined by a per-unit-length self-admittance, Y_C , and a per-unit-length self-impedance, Z_C . The field penetrating the shield has per-unit-length transfer admittance, Y_T , and transfer impedance, Z_T . Transfer parameters define distributed current (I_C) and voltage (V_C) along the inner conductor, given by Eqs. (1) and (2), respectively.

$$E_z(z) = Z_T I_0(z) = \frac{dV_C}{dz} + Z_C I_C \quad (1)$$

$$J_z(z) = -Y_T V_0(z) = \frac{dI_C}{dz} + Y_C V_C \quad (2)$$

Equations (3) and (4) define the transfer admittance and transfer impedance. The transfer admittance is a function of frequency and transfer capacitance, C_T . The transfer impedance (4) is a function of internal transfer impedance, Z_R , transfer inductance, L_T , frequency, and shield diffusion, Z_S .

$$Y_T = j\omega C_T \quad (3)$$

$$Z_T = Z_R + j\omega L_T + Z_S \quad (4)$$

In this paper, we consider two 22-inch-long, commercial single shield cables, which differ for the level of optical coverage: Belden 8240 (95%) and Belden 9201 (78%). Shield diffusion effects are accounted for by $Z_R = R_{gs}(\gamma d_R / \sin(\gamma d_R))$, where $\gamma = \frac{1-j}{\delta} = (1.21 - j1.21) \times 10^{-3} \sqrt{\omega/\omega_0} \text{ inch}^{-1}$; $R_{gs} = \frac{2}{\pi^2 \sigma G_0 \cos(\alpha) d_m d}$; d_m is the average braid diameter; d is the wire diameter; σ is the wire conductivity; α is the braid angle; $G_0 = \frac{mnd}{2\pi d_m}$; m is the number of carriers; n is the number of wires per carrier;

Table 1. Parameters of the Belden 8240 and Belden 9201 cables.

	Belden 8240	Belden 9201
R_{gs} (m Ω /m)	13.34	18.34
d_R (in.)	3.5×10^{-3}	3.47×10^{-3}
C_T (fF/m)	7.30	177.90
L_T (pH/m)	-754.90	-134.60
L_S (pH/m)	$-462.67\sqrt{\omega_0/\omega}$	$-217.67\sqrt{\omega_0/\omega}$
Braid angle ($^\circ$)	24.40	22.00
Strands/carrier	7	5
Shield outer diam. (in.)	0.134	0.130

and skin depth is defined by $\delta = \sqrt{\frac{2}{\omega\mu_0\sigma}} = 8.2 \times 10^{-4}\sqrt{\omega_0/\omega}$, and $\omega_0 = 2\pi \times 10^7$ rad/s. Lastly, $Z_S = (1 + j)\omega L_S$ is assumed to be a forty five degree quantity. Parameter values for each cable are given in Table 1. Both cables share a strand diameter of 0.005 inches, a shield inner diameter of 0.116 inches, a conductor outer diameter of 0.033 inches, and a jacket outer diameter of 0.193 inches.

The distributed transmission-line implementation of a lossy outer shield and inner conductor is shown in Figure 3. In each circuit, a single unit cell is indicated by the blue dashed box.

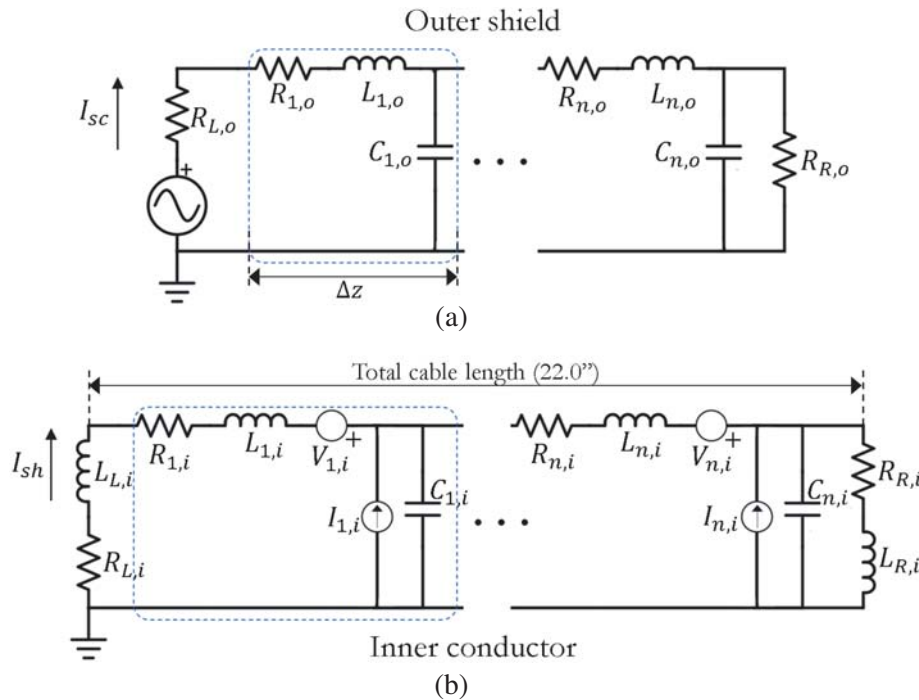


Figure 3. Circuit implementation of the transmission-line models for the (a) outer shield and (b) inner conductor. Blue dashed boxes outline the unit cells of length Δz .

In the outer shield, termination loads are represented by resistors $R_{L,o}$ and $R_{R,o}$, and set to $\sqrt{L_0/C_0}$ to mimic matched loads, with $L_0 = (\mu_0/2\pi)\cosh^{-1}(h/r)$ and $C_0 = (2\pi\epsilon_0)/\cosh^{-1}(h/r)$, where h is the distance of the cable from the ground plane in the experiment, and r is the radius of the outer shield. In general, more complex loads can be considered. The inductance of the n^{th} unit cell is defined as $L_{n,o} = (\text{Im}(Z_e)/\omega)\Delta z$, where $Z_e = Z_{shield} + j\omega L_0$ and N is the total number of stages used and $\Delta z = l/N$, with l representing the total cable length. A rough approximation for the shield impedance

(neglecting proximity effects of the various shield conductors), Z_{shield} , is defined by Eq. (5), where d_w is the diameter of the wire, $G_{shield} = \sqrt{j\omega\mu_0\sigma}$, and $J_0(\rho)$ and $J_1(\rho)$ are the Bessel functions of order 0 and 1, respectively; note because of the lossy terminating loads (in this case matched) this shield impedance has almost no effect on the current. The capacitance of the n th unit cell is defined as $C_{n,o} = C_0\Delta z$. The resistance of the n th unit cell is determined by $R_{n,o} = \text{Re}(Z_e)\Delta z$.

$$Z_{shield} = R_{gs} \cdot \frac{G_{shield}d_w}{2} \cdot \frac{J_0\left(\frac{G_{shield}d_w}{2}\right)}{2J_1\left(\frac{G_{shield}d_w}{2}\right)} \quad (5)$$

In the inner conductor, the inductance and capacitance of the n th unit cell are defined as $L_{n,i} = (\mu_0/2\pi) \log(\frac{d_{si}+d_w}{d_{ic}})$ and $C_{n,i} = 2\pi\epsilon_0\epsilon_1/\log(\frac{d_{si}+d_w}{d_{ic}})$, respectively, where d_{si} is the inner diameter of the shield, d_{ic} is the diameter of the inner conductor, and ϵ_1 is the relative permittivity of the region between shield and inner conductor, with a value of 2.3. The resistance of the n th unit cell is determined by $R_{n,i} = R_0\sqrt{\omega/\omega_0}$.

During the simulation of the outer shield, current flowing through the inductor and voltage across the capacitor are extracted from each unit cell. These values are used to calculate the distributed sources on the inner conductor as shown in the right panel of Figure 2. In other words, the distributed sources are defined as $V_{n,i} = Z_T I_{n,o}$ and $I_{n,i} = -Y_T V_{n,o}$, where $I_{n,o}$ is the current flowing through the $L_{n,o}$ inductor and $V_{n,o}$ is the voltage across the $C_{n,o}$ capacitor. For brevity, we compute the ratio of I_{sh} to I_{sc} in Fig. 3 to determine the shielding effectiveness (note that other locations along the cable can also be used):

$$SE = 20\log(I_{sh}/I_{sc}) \quad (6)$$

3. COMPARISON OF SHIELDING EFFECTIVENESS RESULTS BETWEEN THE CIRCUIT MODEL AND ANALYTIC SOLUTIONS

We now consider the two commercial cables mentioned in Sec. 2. Parameters for each cable are listed in Table 1.

A convergence study was undertaken for each cable to determine how many stages N are needed to achieve good accuracy when compared to the analytical model in [1]. This study is reported in Figure 4 for the Belden 8240 cable and in Figure 5 for the Belden 9201 cable. Shielding effectiveness in Eq. (6) is plotted versus frequency.

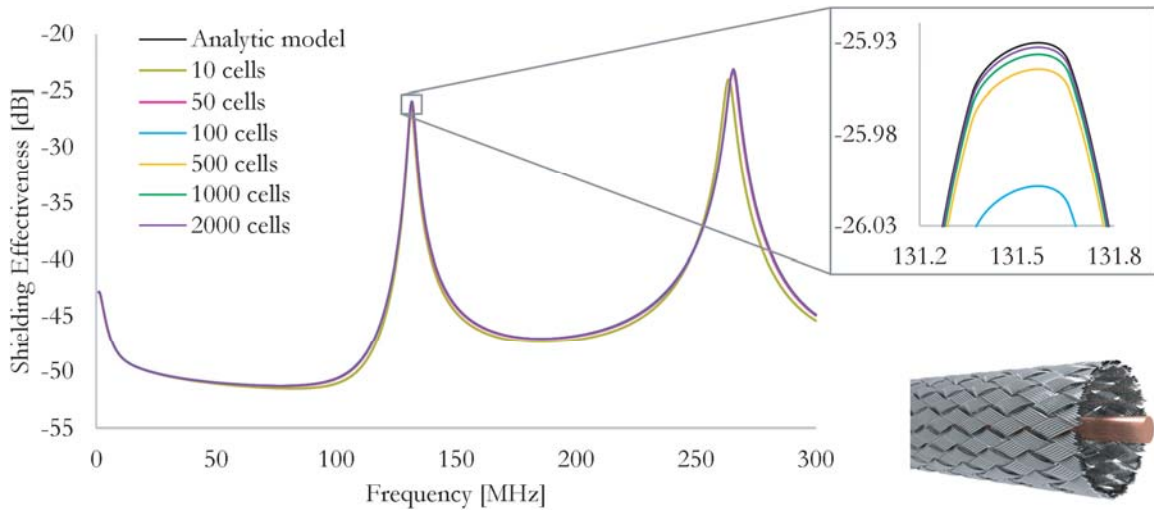


Figure 4. Spectral SE is plotted for the Belden 8240 cable. The inset shows a zoomed region around the first peak and an illustration of the cable geometry.

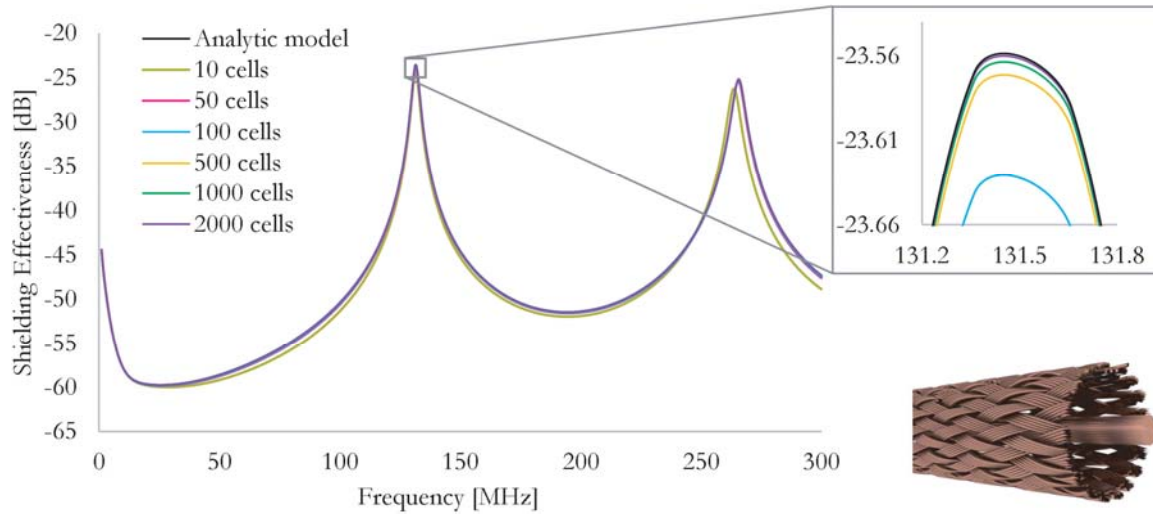


Figure 5. Spectral SE is plotted for the Belden 9201 cable. The inset shows a zoomed region around the first peak and an illustration of the cable geometry.

As the number of unit cells increases, the shielding effectiveness of the Belden 8240 circuit model converges with that predicted by the analytic model. For a geometry with 2000 unit cells, larger than 99.99% agreement of the peak SE value is achieved. Similarly, the peak SE value predicted by the Xyce model for the Belden 9201 cable quickly converges to within 0.03% of the peak SE value predicted by the analytic model. Note, however, that 50 cells would be sufficient to model both cables.

4. EXPERIMENTAL VALIDATION OF THE PROPOSED CIRCUIT MODEL

Given the solid agreement between the analytic and numerical circuit models, an experiment (whose setup is shown in Figure 6) was performed to validate the results.

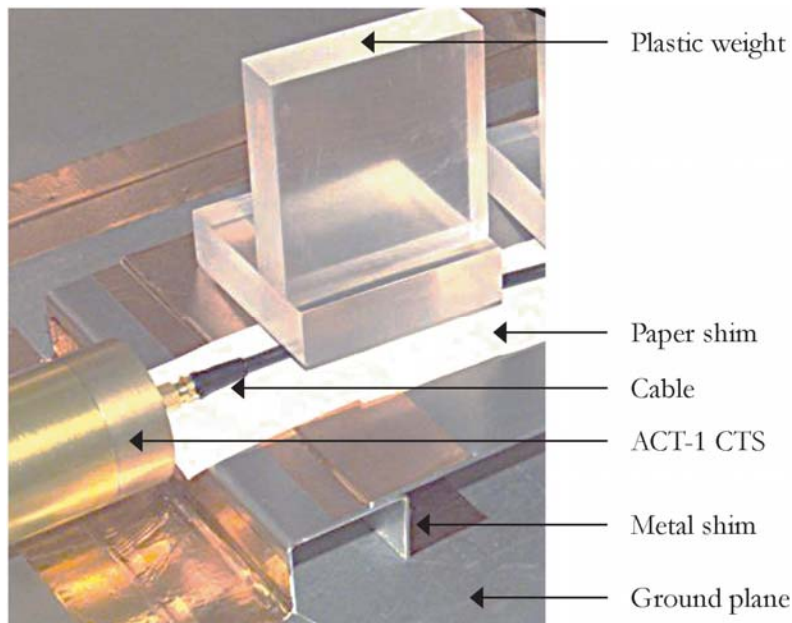


Figure 6. The experiment layout for gathering SE data.

The experiment utilized 22-inch cables, each terminated with SubMiniature version A (SMA) connectors at each end. To reduce leakage into the inner conductor from the shield termination, the outer shield is soldered to the connector. Shielding attenuation provided by the outer shield of the braided cable is measured using an ACT-1 Cable Test System (CTS) [16]. This cable tester was constructed long ago to enable testing of shielding effectiveness (cable current ratio in this case) for arbitrary cables, including flat cables and branched systems, and mimics typical cable routing above a ground plane chassis. It also exercised cable systems at the first resonances. Alternative measurement systems can be found in [17] and [18].

The test cable is aligned with the centerline of the CTS using metal and paper shims. Plastic weights are used to keep the cable flat against the shims to maintain an impedance value of 50Ω . Once the cable is properly aligned, the CTS is calibrated and reproducibility measurements are taken.

With five measurements per cable, variations in the measured shielding effectiveness for a given cable are summarized with error analysis, represented in Figure 7 by error bars. The circuit model, composed of 2000 unit cells, is plotted with a red dashed line. Inserts depict photographs of the braided shields under analysis.

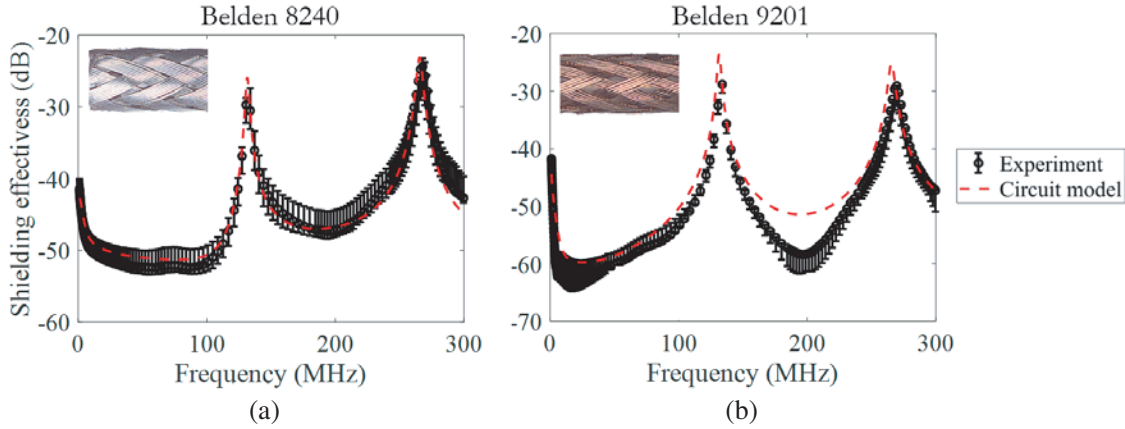


Figure 7. Spectral SE is plotted comparing the circuit model to the experiment results for (a) the Belden 8240 and (b) the Belden 9201 cables.

The Belden 8240 comparison shows strong agreement in amplitude and spectral location of the shielding effectiveness peaks. Similar agreement between SE peak amplitude and spectral location is seen in the comparison of the Belden 9201 cable. Discrepancies in the Belden 9201 response are likely due to near-cancellation of the contribution to the transfer impedance from the porpoising and the braid hole penetration.

5. CONCLUSION

The upset of electronic circuits can be mitigated by the use of electromagnetic shielding, such as braided shields. Knowledge of the geometry of the braided shield enables equivalent circuit analysis for prediction of shielding effectiveness. In this work, we have demonstrated strong agreement between an analytic transmission-line model and numerical circuit analysis tools, representing a step towards multi-physics electromagnetic and circuit simulations. In future work, we will pursue further analyses of end-to-end simulations [15] using the circuit model developed here to translate the exterior environment to an assessment on the electronic system performance of resonant cavities containing cables. Validity of the circuit model was further supported via comparison to experimental data.

ACKNOWLEDGMENT

Sandia National Laboratories is a multimission laboratory managed and operated by National Technology and Engineering Solutions of Sandia, LLC, a wholly owned subsidiary of Honeywell

International, Inc., for the U.S. Department of Energy's National Nuclear Security Administration under contract DE-NA-0003525. This paper describes objective technical results and analysis. Any subjective views or opinions that might be expressed in the paper do not necessarily represent the views of the U.S. Department of Energy or the United States Government.

REFERENCES

1. Campione, S., L. I. Basilio, L. K. Warne, and W. L. Langston, "Shielding effectiveness of multiple-shield cables with arbitrary terminations via transmission line analysis," *Progress In Electromagnetics Research C*, Vol. 65, 93–102, 2016.
2. Casey, K. F., "Electromagnetic shielding behavior of wire-mesh screens," *IEEE Trans. on Elec. Comp.*, Vol. 30, No. 3, 298–306, 1988.
3. Denny, H. W. and K. R. Shouse, "EMI shielding of conductive gaskets in corrosive environments," *IEEE Int. Symp. on Elec. Comp.*, 20–24, Washington, D.C., 1990.
4. Klinkenbusch, L., "On the effectiveness of enclosures," *IEEE Trans. on Elec. Comp.*, Vol. 47, No. 3, 589–601, 2005.
5. Vance, E. F., "Shielding effectiveness of braided shields," *IEEE Trans. on Elec. Comp.*, Vol. 17, No. 2, 71–77, 1975.
6. Vance, E. F., *Coupling to Shielded Cables*, R. E. Krieger, 1987.
7. Lee, K. S. H., *EMP Interaction: Principles, Techniques, and Reference Data*, Hemisphere Publishing Corp., Washington, 1986.
8. Celozzi, S., R. Araneo, and G. Lovat, *Electromagnetic Shielding*, John Wiley and Sons, 2008.
9. Tesche, F. M., M. V. Ianoz, and T. Karlsson, *EMC Analysis Methods and Computational Models*, John Wiley and Sons Inc., New York, 1997.
10. *Xyce Parallel Circuit Simulator*, <http://xyce.sandia.gov>.
11. Kley, T., "Optimized single-braided cable shields," *IEEE Trans. on Elec. Comp.*, Vol. 35, 1–9, 1993.
12. Warne, L. K., W. L. Langston, L. I. Basilio, and W. A. Johnson, "First principles cable braid electromagnetic penetration model," *Progress In Electromagnetics Research B*, Vol. 66, 63–89, 2016.
13. Campione, S., L. K. Warne, W. L. Langston, W. A. Johnson, R. S. Coats, and L. I. Basilio, "Multipole-based cable braid electromagnetic penetration model: Electric penetration case," *IEEE Trans. on Elec. Comp.*, Vol. 60, No. 2, 444–452, 2018.
14. Campione, S., L. K. Warne, W. L. Langston, and L. I. Basilio, "First principles model of electric cable braid penetration with dielectrics," *Progress In Electromagnetics Research C*, Vol. 82, 1–11, 2018.
15. Campione, S., L. K. Warne, and W. L. Langston, "Translation of exterior electromagnetic environment to pin-level voltages and currents on cables," Sandia National Laboratories Report, SAND2018-12274, Albuquerque, NM, USA, 2018.
16. Warne, L. K., L. I. Basilio, W. L. Langston, K. C. Chen, H. G. Hudson, M. E. Morris, S. L. Stronach, W. A. Johnson, and W. Derr, "Electromagnetic coupling into two standard calibration shields on the Sandia cable tester," Sandia National Laboratories Report, SAND2014-0842, Albuquerque, NM, USA, 2014.
17. Fang, C. H., S. Q. Zheng, H. Tan, D. G. Xie, and Q. Zhang, "Shielding effectiveness measurements on enclosures with various apertures by both mode-tuned reverberation chamber and GTEM cell methodologies," *Progress In Electromagnetics Research B*, Vol. 2, 103–114, 2008.
18. "IEEE Standard Method for Measuring the Effectiveness of Electromagnetic Shielding Enclosures," *IEEE Std 299-2006 (Revision of IEEE Std 299-1997)*, 1–52, Feb. 28, 2007